Hindawi Publishing Corporation
Mathematical Problems in Engineering
Volume 2010, Article ID 618231, 14 pages
doi:10.1155/2010/618231

Research Article

Nonlinear Time-Varying Spectral Analysis: HHT and MODWPT

Pei-Wei Shan and Ming Li

School of Information Science & Technology, East Normal University, No. 500, Dong—Chuan Road, Shanghai 200241, China

Correspondence should be addressed to Pei-Wei Shan, midoban43@yahoo.com.cn

Received 31 January 2010; Accepted 19 March 2010

Academic Editor: Cristian Toma

Time-frequency distribution has received a growing utilization for analysis and interpretation of nonlinear and nonstationary processes in a variety of fields. Among them, two methods, such as, the empirical mode decomposition (EMD) with Hilbert transform (HT) which is termed as the Hilbert-Huang Transform (HHT) and the Hilbert spectrum based on maximal overlap discrete wavelet package transform (MODWPT), are fairly noteworthy. Comparisons of HHT and MODWPT in analyzing several typical nonlinear systems and examinations of the effectiveness using these two methods are illustrated. This study demonstrates that HHT can provide comparatively more accurate identifications of nonlinear systems than MODWPT.

1. Introduction

Time-frequency (TF) analysis has experienced a number of qualitative and quantitative changes during the last three decades, and has gradually received growing attentions and further applications in a variety of fields such as radar, water waves [1], fault diagnose, geophysics, and biological signals. However, most traditional signal processing methodologies, developed under rigorous mathematical rigor, are based on linear and stationary assumptions. As the data from the real world are generally neither linear nor stationary, the traditional data analysis methods aimed at linear and stationary signals and processes are becoming glaringly inadequate. In recent years, several new methods have been introduced to analyze nonlinear and nonstationary data. For instance, spectrogram and Wigner-Ville distribution [2] were designed for linear but nonstationary data. In addition, to accommodate for nonlinear but stationary and deterministic processes, Tong (1990), Kantz, and Schreiber (1997), and Diks (1999) raised various time-series-analysis methods [3–5].

Whereas most signals and processes, either natural or artificial ones, are most probably be simultaneously nonlinear and nonstationary. Thus this makes finding a suitable approach to such kind of data a dread in a way.

Huang and Shen put forward that all the analyses in terms of a priori established basis have drained all the physics out of the analyzed results, because any a priori basis could not possibly fit all the variety of data from different driving mechanisms [6]. As the ultimate goal for data analysis is not only to find the mathematical properties of data, but also to excavate the physical insights and implications hidden in the data, the adaptivity becomes absolutely necessary for nonlinear and nonstationary data. Following with the two historical views of nonlinear mechanics of Fourier and of Poincaré, Huang et al. proposed the Hilbert view based on a new method, called empirical mode decomposition (EMD) and Hilbert spectral analysis, which is termed as the Hilbert-Huang Transform (HHT) [7]. The approach of combining EMD and HT differs from the Fourier transform and wavelet analysis. It provides a faithful representation for the nonlinear and nonstationary data analysis. The EMD is conceptualized as an alternative means to separate a multicomponent signal into its monocomponent constituents through a progressive sifting process to yield an empirical base consisting of intrinsic mode function (IMF) components. To ensure that these IMFs have the well-behaved Hilbert transform and conform to a narrowband condition, more definitive stopping criteria such as max sifting iteration are defined. In this way, the data are expanded in a basis derived from the data itself.

Recently, the EMD algorithm, acting as a manner with highly data-driven characteristic of data decomposition, plays a role of either nonlinear or nonstationary processes. With these nice properties, the EMD has been used to calculate the Hurst index of long-range dependence processes (LRD) and network traffic [8], additionally, being an approach of synthesizing fractional processes [9]. In a number of studies, the combination of EMD and HT has been applied and advocated in a variety of problems covering geophysical [10], biomedical engineering [11], and also fluid mechanics as nonlinear water waves and turbulence data [12]. Although several problems still exist in the EMD and the associated Hilbert transform, such that the EMD method may produce mode mixing for some signals [13, 14], the EMD + HT owes strength of being data dependent and provides a potentially viable method and validity of both nonlinear and nonstationary data analyses. Furthermore, it offers a new sight for nonlinear and nonstationary signal processing, that is, individual component signal with physically meaningful instantaneous frequency can be obtained by appropriate signal decomposition method.

Wavelet transforms are one of the fast-evolving mathematical and signal processing tools [15, 16]. A wavelet transform is complete, orthogonal (in the discrete form), and local [17]. A continuous wavelet transform (CWT) decomposes a function by band-pass filtering of the original signal at different bandwidths, while a discrete wavelet transform (DWT) is implemented by using quadrature mirror filter (QMF) banks [18]. The basic operation of wavelet transform consists of the procedures of dilation and translation [19, 20], which lead to a multiscale analysis of a signal. All these vital advantages make wavelet transforms capable of analyzing nonlinear and nonstationary signals. Nevertheless, the deficiencies including the interference terms, border distortion, and energy leakage may generate a lot of undesired small spikes all over the frequency scales and make the results confusing and difficult to be interpreted. To deal with these shortcomings, Olhede and Walden developed another self-adaptive wavelet-based algorithm also via Hilbert transform, namely, maximal-overlap discrete wavelet packet transform (MODWPT) [21]. The ordinary DWT requires the sample size to be exactly a power of 2 for the full transform [22]. Besides, the scaling coefficient of

DWT is not circularly shift equivariant. By avoiding down sampling, MODWPT overcomes these disadvantages of DWT. With optimum decomposition scale and disjoint dyadic decomposition, the complicated signal could be decomposed into a number of components with instantaneous frequencies physically meaningful at different levels. Furthermore, each single component obtained by MODWPT has desirable statistical characteristics, which are desirable properties to deal with nonstationary time series in practice [21].

Duffing equation, Lorenz system, and Rössler system are three of the typical nonlinear examples. The network traffic data is also one kind of practical nonlinear processes [23–30]. Several TF analyses and spectral analyses in network traffic have been used [31]. To discuss the applicability of nonlinear data analysis on HHT and on MODWPT, we will enumerate these several typical nonlinear systems and examine the effectiveness of these two methods in the following representation. The organization of this paper is given as follows. The rationale of HHT and MODWPT will be elaborated separately in Sections 2 and 3. Characteristics of three typical nonlinear systems using HHT and MODWPT will be discussed in Section 4 and the efficiency of each approach will also be demonstrated. In Section 5, we give the future works that are under investigation and exploration. Finally, we will offer the conclusion in Section 6.

2. Rationale of HHT

The development of HHT provides an alternative view of the time-frequency-energy paradigm of nonlinear and nonstationary data. To examine data from real-world nonlinear and nonstationary processes, the detailed dynamics in the processes from the data need to be determined because the intrawave frequency modulation, which indicates the instantaneous frequency changes within one oscillation cycle, is one of the typical characteristics of a nonlinear system. As Huang et al. [7] pointed out, the intrafrequency variation is the hallmark of nonlinear systems. One way to express the nonlinearity is to find instantaneous frequency, which reveals the intrawave frequency modulations. But actually, the detailed frequency representation cannot be obtained from a priori approach hampered by a collection of the endless harmonics [6]. Thus, as an easier approach, the Hilbert Transform is used, which is defined as

$$y(t) = \frac{1}{\pi} P \int_{-\infty}^{\infty} \frac{x(\tau)}{t-\tau} d\tau, \tag{2.1}$$

where P is the Cauchy principal value of the singular integral and in which $y(t)$ is the Hilbert transform of the function $x(t)$. The analytic signal is defined as

$$z(t) = x(t) + iy(t) = a(t)e^{i\theta(t)}, \tag{2.2}$$

where

$$a(t) = \sqrt{x^2 + y^2}, \qquad \phi(t) = \arctan\left(\frac{y}{x}\right), \tag{2.3}$$

where $a(t)$ is the instantaneous amplitude, and ϕ is the instantaneous phase function. The instantaneous frequency is

$$\omega = \frac{d\phi}{dt}. \tag{2.4}$$

The purpose is to separate function $x(t)$ into a set of nearly monocomponent signals called IMFs. An IMF is a single frequency component within the length of the signal. The way of extracting instantaneous frequencies is called EMD [7].

2.1. Empirical Mode Decomposition

Physically speaking, the necessary conditions to define a meaningful instantaneous frequency are that the signal must be symmetric concerning the local zero mean, and have the same numbers of zero crossings and extrema. This means that, in an IMF function, the number of extrema and the number of zero crossings must be either equal or different at most by one in the whole data set, and the mean value of the envelope defined by the local maxima and the envelope defined by the local minima is zero at every point. All these conditions are so strict that the determined IMF may not satisfy them precisely. Consequently, the resultant IMF is nearly a monocomponent function.

The EMD is developed based on the assumption that any signal consists of a set of different IMFs. The procedures to decompose signal $x(t)$ can be enumerated as following steps.

(a) Find all the local maxima from $x(t)$ and connect them with the cubic spline to form the upper envelope denoted by $x_{\text{up}}(t)$.

(b) Find all the local minima from $x(t)$ and connect them with the cubic spline to form the lower envelope denoted by $x_{\text{low}}(t)$.

(c) Let the mean $m_1(t) = [x_{\text{up}}(t) + x_{\text{low}}(t)]/2$.

(d) Subtract the difference $h_1(t)$ between the signal $x(t)$ and the mean $m_1(t)$: $h_1(t) = x(t) - m_1(t)$.

(e) Ideally, the difference $h_1(t)$ should be an IMF. Repeat step (d) as a sifting process by treating $h_1(t)$ as the signal: $h_{11}(t) = h_1(t) - m_{11}(t)$.

(f) Repeat the sifting process k times until $h_{1k}(t)$ becomes a true IMF as

$$h_{1k}(t) = h_{1(k-1)}(t) - m_{1(k-1)}(t), \tag{2.5}$$

and it is designated as: $c_1(t) = h_{1k}(t)$.

(g) The criterion suggested by Huang for stopping the sifting process is

$$SD = \sum_{t=0}^{N} \left[\frac{\left| h_{1(k-1)}(t) - h_{1k}(t) \right|^2}{h^2{}_{1(k-1)}(t)} \right], \tag{2.6}$$

and the SD value is regularly 0.2~0.3.

(h) Remove $c_1(t)$ from the rest of the signal by $r_1(t) = x(t) - c_1(t)$ and treat $r_1(t)$ as a new signal and repeating step (a) to (f) as described above. Thus, we can obtain a series of IMFs c_i $(i = 1, 2, ..., n)$ and the final residue $r_n(t)$.

Summing up all the IMFs and the final residue, we should be able to reconstruct the original signal $x(t)$ by [7]

$$x(t) = \sum_{i=1}^{n} c_i(t) + r_n(t). \tag{2.7}$$

Then, the HT of $c_i(t)$ yields

$$x(t) = \mathrm{Re}\left(\sum_{i=1}^{n} a_i(t) e^{j\phi_i(t)}\right) + r_n(t) = \mathrm{Re}\left(\sum_{i=1}^{n} a_i(t) e^{j\int \omega_i(t)dt}\right) + r_n(t). \tag{2.8}$$

In the polar coordinates system, $x(t)$ is expressed by

$$x(t) = \mathrm{Re}\left(\sum_{i=1}^{n} a_i(t) \exp\left[j \int \omega_i(t)dt\right]\right) + r_n(t). \tag{2.9}$$

Practically, the residue $r_n(t)$ can be ignored.

Let $a_i(\omega, t)$ be the combination of the amplitude $a_i(t)$ and the instantaneous frequency $\omega_i(t)$ of the ith IMF. The HHT of $x(t)$ is given by

$$\mathrm{HHT}(\omega, t) = \sum_{i=1}^{n} a_i(\omega, t). \tag{2.10}$$

3. Hilbert Spectrum via MODWPT

Assume that we sample a continuous-time signal at intervals $\Delta t = 1$ to a sequence of the observation $X = [X_0, X_1, \ldots, X_{N-1}]$ and N is a power of 2. For the class of discrete compactly supported Daubechies wavelets, we denote the scaling (low-pass) filter by $\{g_l : l = 0, \ldots, L-1\}$ and the wavelet (high-pass) filter by $\{h_l : l = 0, \ldots, L-1\}$. These even-length filters satisfy

$$\sum_{l=0}^{L-1} g_l^2 = 1, \qquad \sum_{l=0}^{L-1} g_l g_{l+2n} = \sum_{l=-\infty}^{\infty} g_l g_{l+2n} = 0 \tag{3.1}$$

for all nonzero integers n, and are related by being quadrature mirror filters:

$$h_l = (-1)^l g_{L-l-1} \quad \text{or} \quad g_l = (-1)^{l+1} h_{L-l-1} \quad \text{for } l = 0, \ldots, L-1. \tag{3.2}$$

For $t = 0, \ldots, N-1$, the jth level wavelet and scaling coefficients are given by

$$\begin{aligned} V_{j,t} &= \sum_{l=0}^{l-1} g_l V_{j-1,(2t+1-l) \bmod N_j - 1} \quad (t = 0, \ldots, N_j - 1), \\ W_{j,t} &= \sum_{l=0}^{l-1} h_l V_{j-1,(2t+1-l) \bmod N_j - 1} \quad (t = 0, \ldots, N_j - 1), \end{aligned} \tag{3.3}$$

where mod means modulus after division.

The maximal overlap discrete wavelet transform (MODWT) can be considered as a revised version of the DWT [21]. As previously mentioned, the DWT of level j restricts the sample size to a power of 2. However, the MODWT of level j is well defined for any sample size. To conserve energy, we define

$$\tilde{g}_l = \frac{g_l}{\sqrt{2}}, \qquad \tilde{h}_l = \frac{h_l}{\sqrt{2}}. \tag{3.4}$$

Thus, (3.1) becomes

$$\sum_{l=0}^{L-1} \tilde{g}_l^2 = \frac{1}{2}, \qquad \sum_{l=0}^{L-1} \tilde{g}_l \tilde{g}_{l+2n} = \sum_{l=-\infty}^{\infty} \tilde{g}_l \tilde{g}_{l+2n} = 0 \tag{3.5}$$

and the quadrature mirror filters are defined likewise

$$\tilde{h}_l = (-1)^l \tilde{g}_{L-l-1} \quad \text{or} \quad \tilde{g}_l = (-1)^{l+1} \tilde{h}_{L-l-1} \quad \text{for } l = 0, \ldots, L-1. \tag{3.6}$$

The MODWT creates new filters at each stage by inserting $2^{j-1} - 1$ zeros between the elements of $\{\tilde{g}_l\}$ and $\{\tilde{h}_l\}$ to avoid downsampling. The MODWT pyramid algorithm generates the MODWT wavelet coefficients $\{W_{j,t}^{(M)}\}$ and the scaling coefficients $\{V_{j,t}^{(M)}\}$, respectively by

$$\begin{aligned} V_{j,t} &= \sum_{l=0}^{l-1} \tilde{g}_l V_{j-1,(t-2^{j-1}l) \bmod N} \quad (t = 0, \ldots, N_j - 1), \\ W_{j,t} &= \sum_{l=0}^{l-1} \tilde{h}_l V_{j-1,(t-2^{j-1}l) \bmod N} \quad (t = 0, \ldots, N_j - 1). \end{aligned} \tag{3.7}$$

The coefficients at level j and frequency-index n can be expressed as $W_{j,n} = \{W_{j,n,t}, t = 0, \ldots, N-1\}$, and then we produce $\{W_{j,n,t}\}$ using

$$W_{j,n,t} = \sum_{l=0}^{l-1} \widetilde{f}_{n,l} W_{j-1,[n/2],(t-2^{j-1}l) \bmod N} \quad (t = 0, \ldots, N_j - 1), \tag{3.8}$$

when n mod 4 = 0 or 3, $\widetilde{f}_{n,l} = \widetilde{g}_l$; when n mod 4 = 1 or 2, $\widetilde{f}_{n,l} = \widetilde{h}_l$.

For any signal, the analytic form can be represented as

$$s(t) = W_{j,n}(t) + jH\left[W_{j,n}(t)\right]. \tag{3.9}$$

Then the instantaneous amplitude is denoted by

$$a_{j,n}(t) = \sqrt{W_{j,n}^2(t) + H^2\left[W_{j,n}(t)\right]}, \tag{3.10}$$

and the instantaneous phase function is

$$\phi_{j,n}(t) = tg^{-1} \frac{H\left[W_{j,n}(t)\right]}{W_{j,n}(t)}. \tag{3.11}$$

Accordingly, the instantaneous frequency is

$$f_{j,n}(t) = \frac{1}{2\pi} \phi'_{j,n}(t). \tag{3.12}$$

4. Nonlinear System

Generally speaking, the instantaneous frequency changes within one oscillation cycle for nonlinear systems, and can be used to describe intrawave frequency modulation. To discuss the characteristics of data from a nonlinear system by EMD + HT and MODWPT, we will take several typical examples to aid the discussions.

4.1. Duffing System

The Duffing oscillator under harmonic excitation described by a second-order differential equation is one of the well-known nonlinear examples

$$\frac{d^2x}{dt^2} + x + \varepsilon x^3 = \gamma \cos \omega t, \tag{4.1}$$

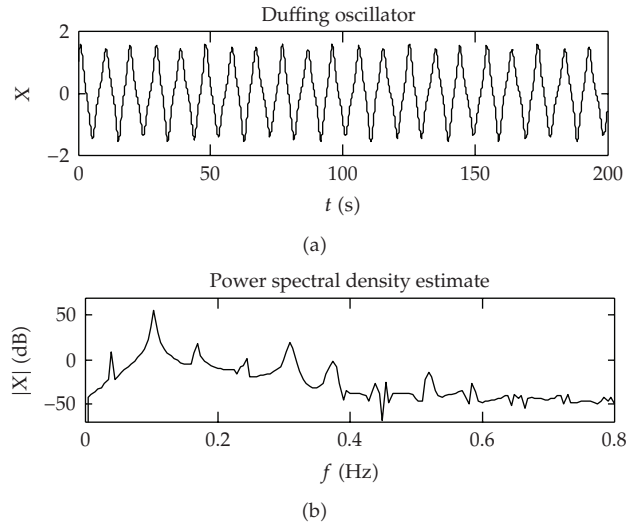

Figure 1: (a) Numerical solution of the Duffing equation (200s). (b) Power spectral density estimate.

where ε, γ = constants, and ω = harmonic forcing frequency. If we rewrite the equation in the following form

$$\frac{d^2x}{dt^2} + \left(1 + \varepsilon x^2\right)x = \gamma \cos \omega t, \tag{4.2}$$

the term in parenthesis could be interpreted as nonlinearity in the stiffness of the oscillator, which will lead to a frequency that is ever changing with amplitude from location to location, and time to time, even within a single period.

Embodied by a Duffing oscillator with $\varepsilon = -1$ and $\gamma = 0.1$, the system is allowed to freely vibrate and with the initial conditions of $x(0) = 1$ and $\dot{x}(0) = 1$, as shown in Figure 1.

After subjected to the EMD, the numerical result yields the IMF components and the corresponding Fourier spectrum of each IMFs as shown in Figure 2, where the first IMF, indicating a concentration of energy near 0.12 Hz, represents the intrinsic frequency of the system. The second IMF, identifying a weak concentration of energy around 0.04 Hz, represents the forcing function, and a low-frequency component, with low energy at 0.017 Hz, represents the very low-intensity subharmonics. Figure 3 illustrates the TF outcome of the Duffing equation using EMD and MODWPT. Apparently, the HHT result reveals the intrinsic frequency clearly, which shows strong introwave frequency modulation, presented as a variable frequency oscillation between 0.06~0.18 Hz. The forcing function is also perfect shown at 0.04 Hz. The low frequency and low amplitude at 0.02 Hz are unexpected but explicable, for they represent the slow aperiodic wobbling of the phase. The Hilbert marginal spectrum of HHT shows the intrawave frequency modulation from 0.06 to 0.18 Hz and the forcing function near 0.04 Hz likewise. Compared to the HHT, while the TF spectrum of MODWPT indicates the frequency oscillation near 0.1 Hz, the forcing function at 0.04 Hz is not displayed, just similar to the Hilbert marginal spectrum on right.

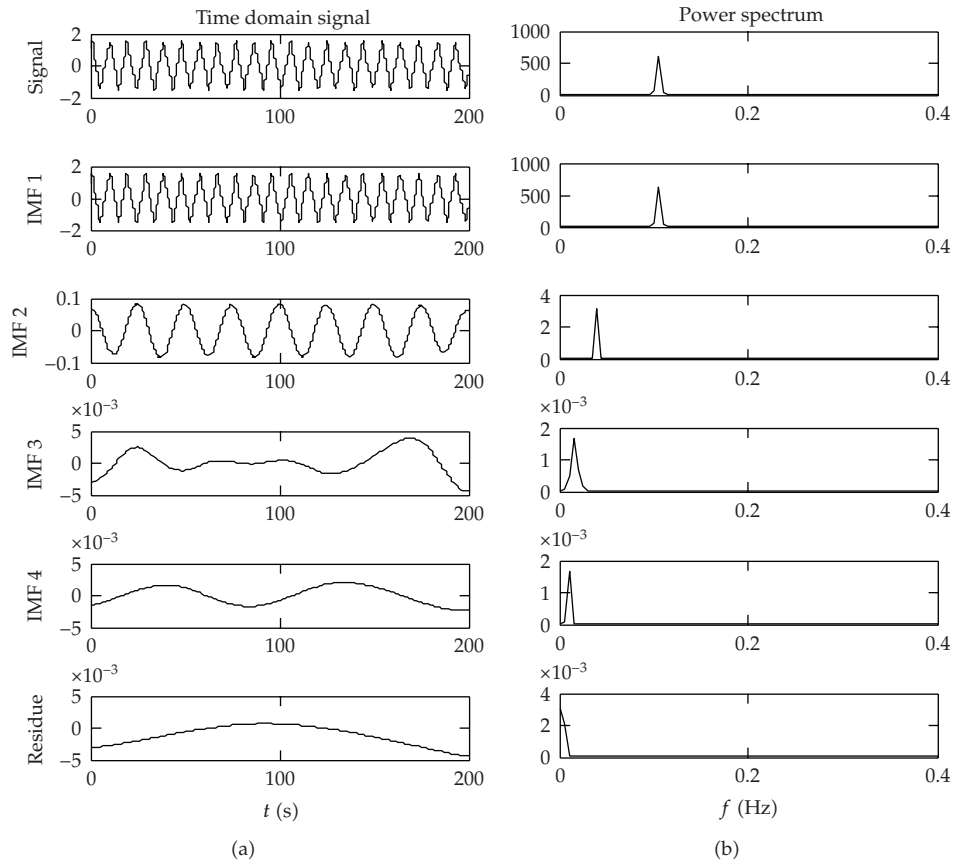

Figure 2: The IMF components of the Duffing equation from EMD in (a) and the corresponding power spectrum in (b).

4.2. Duffing System

The Lorenz system has also been widely studied and is described by

$$\dot{x} = -\sigma(x - y), \qquad \dot{y} = x(r - z) - y, \qquad \dot{z} = -bz + xy, \tag{4.3}$$

where σ, r, and b = positive constants, assumed to be 10, 20, and 3, with initial position of $(10, 0, 0)$. The numerical result is shown in Figure 4. The IMFs are displayed in Figure 5 with the corresponding Fourier spectrum on right. The comparisons of TF resolutions using HHT and MODWPT are provided in Figure 6. The sharp peak that appears at 1.4 Hz in the Fourier spectrum represents the main oscillating frequency.

In the diagram of HHT, the transient nature of both components is perfectly located, with the main component being intrawave modulated and a fairly clear indication of the nonlinear effect of the oscillation. Comparatively speaking, the result of MODWPT is not so satisfactory. Only some blurry frequency components can be recognized near 1.4 Hz. The oscillation of the frequency, supposed to be demonstrating the nonlinearity, is not represented here in the spectrum of the MODWPT.

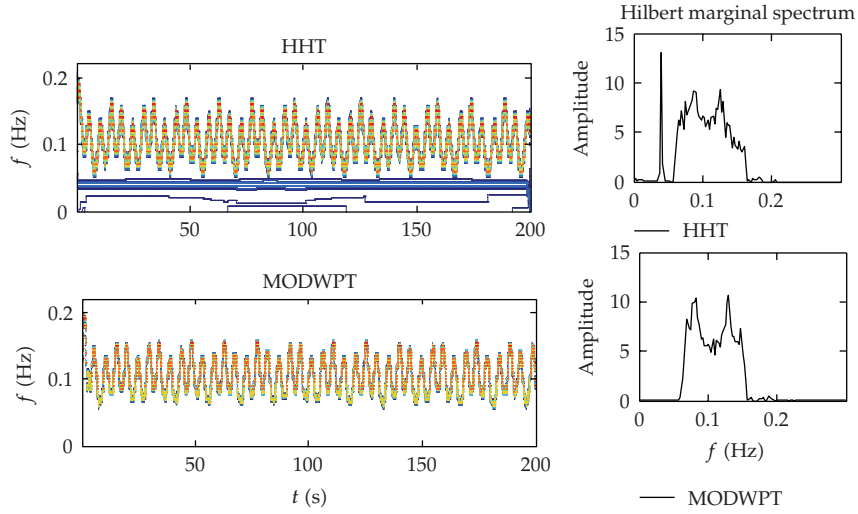

Figure 3: Diagrams at left represent the HHT result and the MODWPT result (at level 3) of the Duffing equation separately; the corresponding Hilbert Marginal spectrum results of EMD and MODWPT are on the right side.

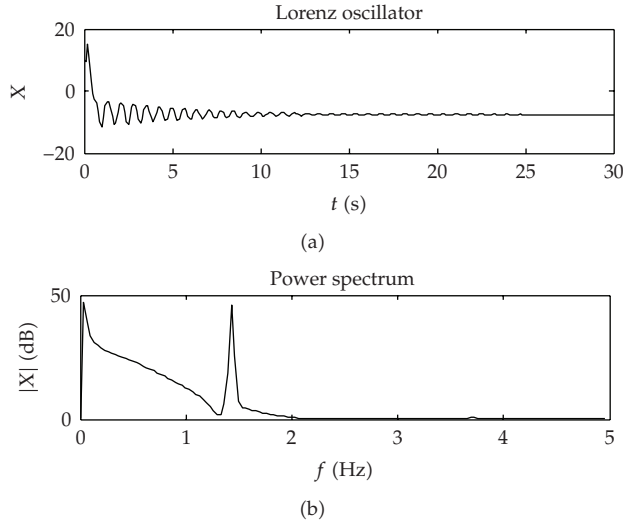

Figure 4: The numerical solution of the Lorenz equation (a) and the Fourier spectrum of the given x-component (b).

4.3. *Duffing System*

Another example investigated here is the Rössler System denoted as

$$\dot{x} = -(y + z), \qquad \dot{y} = x + \frac{1}{5}y, \qquad \dot{z} = \frac{1}{5} + z(x + \mu), \tag{4.4}$$

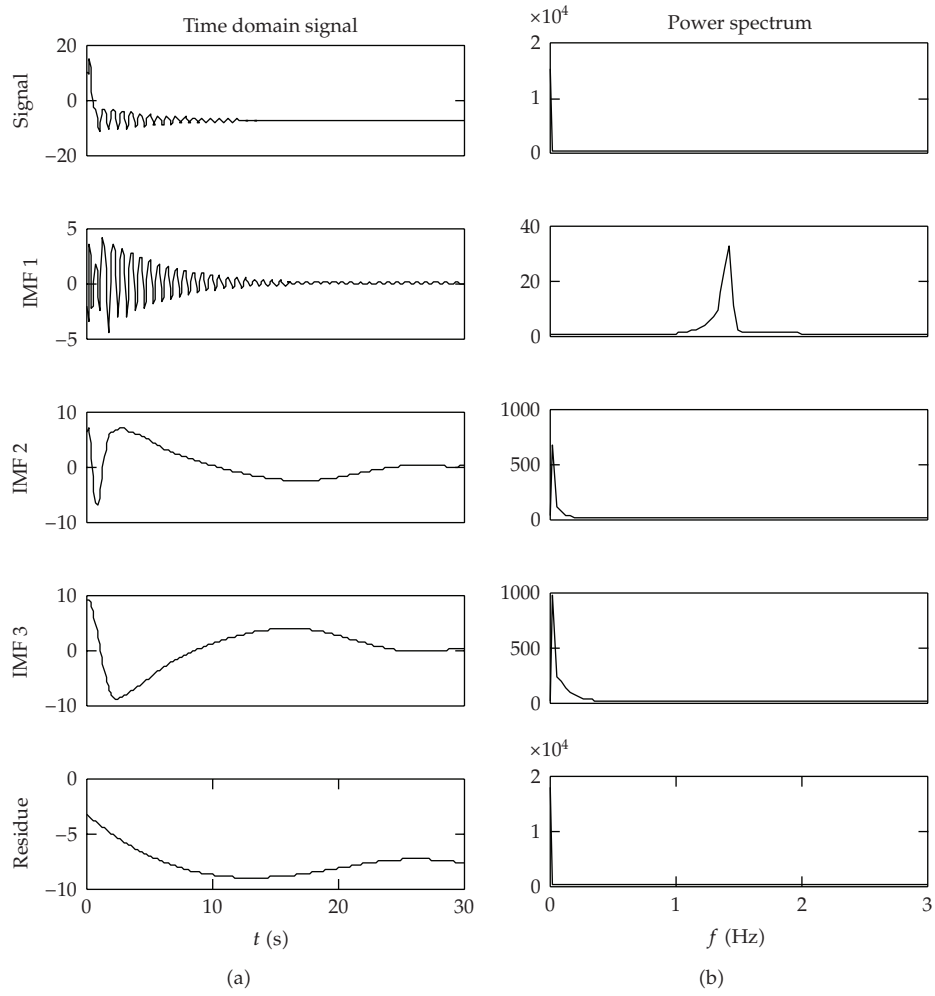

Figure 5: The IMF components of the Lorenz equation from EMD in (a) and the corresponding power spectrum in (b).

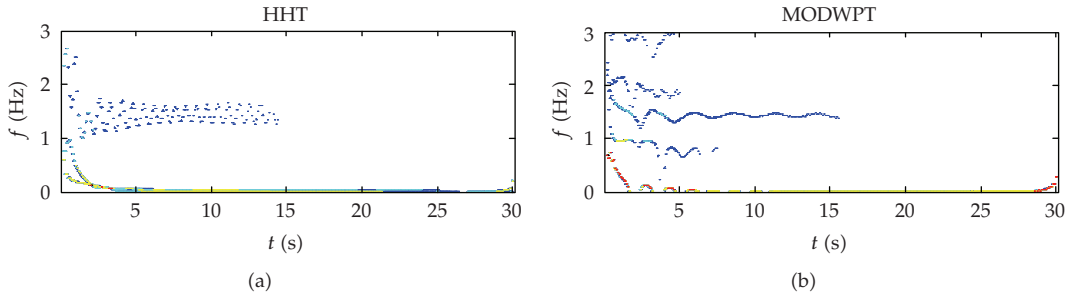

Figure 6: The HHT spectrum (a) and the MODWPT spectrum at level 3 (b) for the Lorenz equation solution.

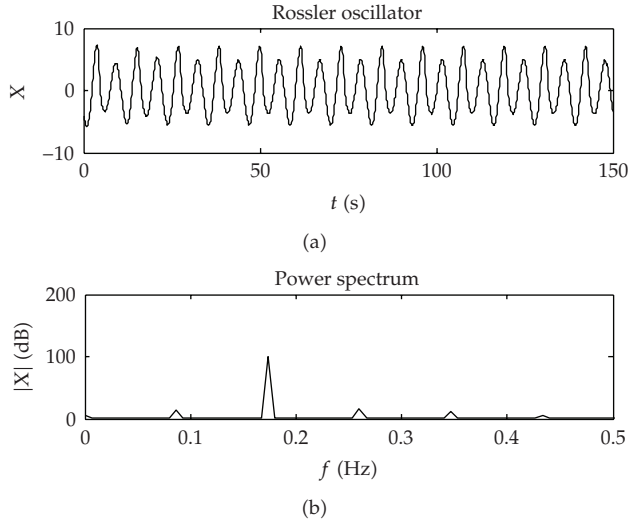

Figure 7: The waveform of the x-component in diagram (a) and The Fourier spectrum of x (b).

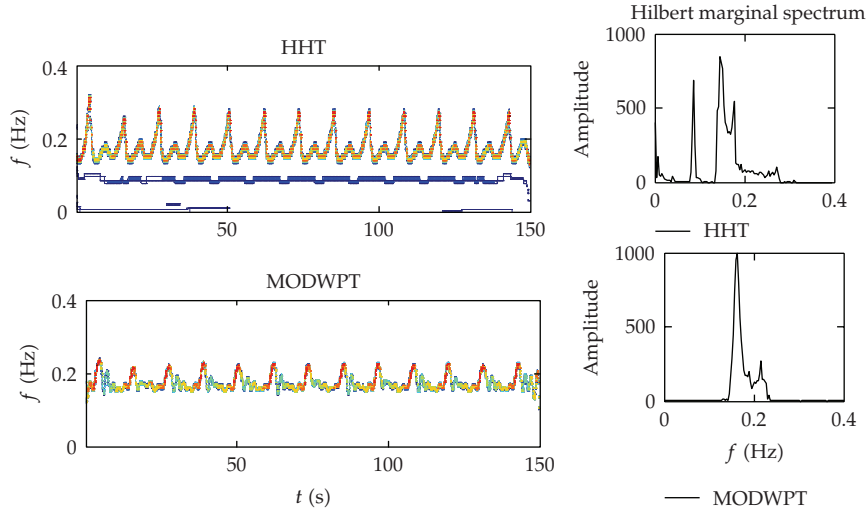

Figure 8: Comparison of the TF distribution of Rossler equation using HHT and MODWPT (level 3) on left and the corresponding marginal spectrum on right.

where μ is a constant parameter which stands for the famous period-doubling event and we let it be $\mu = 3.5$. Also we assume the initial condition to be (−4,4,0). Wave form of the x-component is displayed in Figure 7.

The result of the Fourier spectrum of x-component shows many harmonics at 0.27 Hz, 0.35 Hz, and 0.42 Hz, separately 3 times, 5 times, and 7 times of 0.07 Hz. The HHT spectrum and the MODWPT distribution are given in Figure 8 on the left column. The corresponding Hilbert marginal spectrum of each method is on the right column. The marginal spectrum gives a low-frequency peak and a broad bimodal distribution near the main peak frequency, which indicates a typical distribution of a periodic variable. None of the peaks in the marginal

spectrum agree with the main peak in the Fourier spectrum in Figure 7. Comparatively, the peak near 0.07 Hz in marginal spectrum of HHT does not appear in the marginal spectrum of MODWPT. Similarly, the high bimodal frequency distribution around 0.18 Hz generated by the intrawave frequency modulation in marginal spectrum of MODWPT agrees with these in marginal spectrum of HHT, which indicates the two time scales involved in the period doubling. As these results showed, the EMD decomposed the data into two nonlinear components more successfully than the MODWPT.

5. Future Work

This paper focuses on the performance of nonlinear processes using the HHT and the MODWPT with the aim of bringing a better choice of time-frequency decomposition in nonlinear data analysis. Compared with the HHT, the MODWPT shows some weakness in nonlinear data analysis and the study of identifying the computational burden required by these two methods is still at the exploratory stage.

6. Conclusion

HHT, which decomposes data through EMD, offers a potentially viable method for nonlinear and nonstationary data analysis. Verified by three typical nonlinear systems, the HHT can not only perform and locate main frequency components but also force function frequency details. Furthermore, the intrawave modulation, which is the important characteristic of nonlinear system, can as well be obtained in the distribution of HHT. Compared with the MODWPT that decomposes data into a number of components alike, the EMD gives results much sharper and more supportable to nonlinear system identification.

Acknowledgment

This work was supported in part by the National Natural Science Foundation of China (NSFC) under the project Grants numbers 60573125 and 60873264.

References

[1] M. Li, X. K Gu, and P. W Shan, "Time-frequency distribution of encountered waves using Hilbert-Huang transform," *International Journal of Mechanics*, vol. 1, no. 2, pp. 27–32, 2007.

[2] P. Flandrin, *Time-Frequency/Time-Scale Analysis*, vol. 10 of *Wavelet Analysis and Its Applications*, Academic Press, San Diego, Calif, USA, 1999.

[3] H. Tong, *Nonlinear Time Series Analysis*, Oxford University Press, Oxford, UK, 1990.

[4] H. Kantz and T. Schreiber, *Nonlinear Time Series Analysis*, vol. 7 of *Cambridge Nonlinear Science Series*, Cambridge University Press, Cambridge, UK, 1997.

[5] C. Diks, *Nonlinear Time Series Analysis*, vol. 4 of *Nonlinear Time Series and Chaos*, World Scientific, Singapore, 1999.

[6] N. E. Huang and S. S. Shen, Eds., *Hilbert-Huang Transform and Its Applications*, vol. 5 of *Interdisciplinary Mathematical Sciences*, World Scientific, Singapore, 2005.

[7] N. E. Huang, Z. Shen, S. R. Long, et al., "The empirical mode decomposition and the Hilbert spectrum for nonlinear and non-stationary time series analysis," *Proceedings of the Royal Society London A*, vol. 454, no. 1971, pp. 903–995, 1998.

[8] P. Flandrin and P. Gonçalvès, "Empirical mode decompositions as data-driven wavelet-like expansions," *International Journal of Wavelets, Multiresolution and Information Processing*, vol. 2, no. 4, pp. 477–496, 2004.
[9] P. Shan and M. Li, "An EMD based simulation of fractional Gaussian noise," *International Journal of Mathematics and Computers in Simulation*, vol. 1, no. 4, pp. 312–316, 2007.
[10] N. E. Huang, S. R. Long, and C. C. Tung, "The local properties of transient stochastic data by the phase-time method," in *Computational Methods for Stochastic Processes*, pp. 253–279, 1993.
[11] W. Huang, Z. Shen, N. E. Huang, and Y. C. Fung, "Engineering analysis of biological variables: an example of blood pressure over 1 day," *Proceedings of the National Academy of Sciences of the United States of America*, vol. 95, no. 9, pp. 4816–4821, 1998.
[12] N. E. Huang, "Nonlinear evolution of water waves: Hilbert's view," in *Proceedings of the International Symposium on Experimental Chaos*, W. Ditto, C. Grebogi, E. Ott, et al., Eds., pp. 327–341, World Scientific, Scotland, UK, 2nd edition, 1995.
[13] M. Datig and T. Schlurmann, "Performance and limitations of the Hilbert-Huang transformation (HHT) with an application to irregular water waves," *Ocean Engineering*, vol. 31, no. 14, pp. 1783–1834, 2004.
[14] N. E. Huang and Z. H. Wu, "A review on Hilbert-Huang transform: method and its applications to geophysical studies," *Reviews of Geophysics*, vol. 46, no. 2, 2008.
[15] C. Cattani and J. Rushchitsky, *Wavelet and Wave Analysis as Applied to Materials with Micro or Nanostructure*, vol. 74 of *Series on Advances in Mathematics for Applied Sciences*, World Scientific, Singapore, 2007.
[16] C. Cattani, "Harmonic wavelet approximation of random, fractal and high frequency signals," *Telecommunication Systems*, vol. 43, no. 3-4, pp. 207–217, 2010.
[17] C. Cattani, "Harmonic wavelet analysis of a localized fractal," *International Journal of Engineering and Interdisciplinary Mathematics*, vol. 1, no. 1, pp. 35–44, 2009.
[18] C. Cattani, "Shannon wavelets theory," *Mathematical Problems in Engineering*, vol. 2008, Article ID 164808, 24 pages, 2008.
[19] C. L. Zhang, H. Chen, X. F. Wang, and D.-H. Fan, "Harmonic wavelet analysis of a localized parabolic partial differential equation," *International Journal of Engineering and Interdisciplinary Mathematics*, vol. 1, no. 1, pp. 45–55, 2009.
[20] W.-S. Chen, "Galerkin-Shannon of Debye's wavelet method for numerical solutions to the natural integral equations," *International Journal of Engineering and Interdisciplinary Mathematics*, vol. 1, no. 1, pp. 63–73, 2009.
[21] A. T. Walden and A. Contreras Cristan, "The phase-corrected undecimated discrete wavelet packet transform and its application to interpreting the timing of events," *Proceedings of the Royal Society of London Series*, vol. 454, no. 1976, pp. 2243–2266, 1998.
[22] E. Tsakiroglou and A. T. Walden, "From Blackman—Tukey pilot estimators to wavelet packet estimators: a modern perspective on an old spectrum estimation idea," *Signal Processing*, vol. 82, no. 10, pp. 1425–1441, 2002.
[23] M. Li and S. C. Lim, "Modeling network traffic using generalized Cauchy process," *Physica A*, vol. 387, no. 11, pp. 2584–2594, 2008.
[24] M. Li, "Fractal time series—a tutorial review," *Mathematical Problems in Engineering*, vol. 2010, Article ID 157264, 26 pages, 2010.
[25] M. Li and W. Zhao, "Representation of a stochastic traffic bound," *IEEE Transactions on Parallel and Distributed Systems*. In press.
[26] M. Li and W. Zhao, "Variance bound of ACF estimation of one block of fGn with LRD," *Mathematical Problems in Engineering*, vol. 2010, Article ID 560429, 14 pages, 2010.
[27] M. Li and P. Borgnat, "Foreword to the special issue on traffic modeling, its computations and applications," *Telecommunication Systems*, vol. 43, no. 3-4, pp. 145–146, 2010.
[28] M. Li, W.-S. Chen, and L. Han, "Correlation matching method for the weak stationarity test of LRD traffic," *Telecommunication Systems*, vol. 43, no. 3-4, pp. 181–195, 2010.
[29] M. Li and S. C. Lim, "Power spectrum of generalized Cauchy process," *Telecommunication Systems*, vol. 43, no. 3-4, pp. 291–222, 2010.
[30] M. Li, "Recent results on the inverse of min-plus convolution in computer networks," *International Journal of Engineering and Interdisciplinary Mathematics*, vol. 1, no. 1, pp. 1–9, 2009.
[31] C.-M. Cheng, H. T. Kung, and K.-S. Tan, "Use of spectral analysis in defense against DoS attacks," in *Proceedings of the IEEE Global Telecommunications Conference (GLOBECOM '02)*, vol. 3, pp. 2143–2148, Taipei, China, 2002.